ISSN 0965-545X, Polymer Science, Series A, 2021, Vol. 63, No. 4, pp. 420–428. © Pleiades Publishing, Ltd., 2021.

POLYMER NETWORKS

Preparation and Characterization of Polyoxymethlene/Thermoplastic Polyamide Elastomer Blends Compatibilized by Maleic Anhydride Grafted ABS Copolymer

Ruilong Li[a], Wei Fang[a,b,*], Xiaodong Fan[b,], Zhengwei Jin[a], and Tao Zhou[c]**

[a] *Ningxia Coal Industry Group Corporation, Yinchuan, 750011 China*

[b] *School of Natural and Applied Science, Northwestern Polytechnical University, Xi'an, 710129 China*

[c] *State Key Laboratory of Polymer Materials Engineering, Sichuan University, Chengdu, 610065 China*

**e-mail: wwfang001@126.com*

***e-mail: xfand@126.com*

Received November 2, 2020; revised December 31, 2020; accepted March 5, 2021

Abstract—Polyoxymethylene/thermoplastic polyamide elastomer composites were prepared by using maleic anhydride grafted acrylonitrile-butadiene-styrene copolymer as interfacial compatibilizer via melt extrusion. The compatibility and the properties of blends were studied by the mechanical testing and various physical chemical methods. The notched impact strength and elongation at break of blends were increased significantly after adding of compatibilizer. Simultaneously, the phase structure and crystal shape of the blends were changed. Finally, the elastomer particles were more uniform, and more amorphous regions were produced in the blends.

DOI: 10.1134/S0965545X21040052

INTRODUCTION

Polyoxymethylene (POM) is an excellent engineering thermoplastic, which is considered as an alternative for metals in many applications because of its remarkable mechanical and self-lubricating characteristics [1]. So, it is often used in many extensive applications, such as automobiles, electronic industry, mechanical, industry, constructions and so on [2]. Due to its high degree of crystallinity of about 70%, POM exhibits poor impact strength and is prone to brittle cracking at low temperature. In recent years, many scholars have carried out relevant studies, using different modification methods and additives to improve the toughness of POM products. For examples, the most widely studied is the use of thermoplastic polyurethane (TPU) to improve POM impact strength [3]. Although TPU is a very effective toughening modifier for POM materials [4], thermoplastic polyurethane elastomers also have some obvious shortcomings, such as poor solvent resistance and high temperature resistance is not good enough [5].

To improve these above deficiencies of POM modified by TPU, many scientists have investigated other toughening modifiers and their applications in modified POM [6–16]. For example, Ren [7] has synthesized an acrylate elastomer (ACE) with anti-ultraviolet function to improve the toughness of POM. Zhou [8] has studied mechanical properties and surface morphology of POM modified by a core–shell ACE. Bai [10] has investigated the crystallization and mechanical properties of POM/Poly(ethylene oxide) (PEO) blends, the results showed that when the PEO content was 50%, the notched impact strength of the blend reached 16 kJ/m^2. Wacharawichanant [11] has investigated the morphology and mechanical properties of POM/ABS blends with PP-*g*-MA compatibilizer. The results indicated that PP-*g*-MA could improve the interfacial adhesion of POM/ABS blends due to the domain size of ABS phase decreased after adding PP-*g*-MA. Yang [13] has investigated POM composites toughened by polyolefin elastomer and glycidyl methacrylate grafted high-density polyethylene, the highest impact strength of the sample reached 10.81 kJ/m^2. Yang [14] has used methyl methacrylate-butadiene-styrene copolymer (MBS) as a toughening agent and TPU as a compatibilizer to improve the impact performance of POM. It was found that when the weight ratio of POM/MBS/TPU was 80 : 15 : 10, the notched impact strength of blends can be reached 40 kJ/m^2. Li [15] has prepared POM blends by the star-structured hyper branched polyester, the impact strength of blends could increase nearly 50%. In addition to above reports, the author of this article has studied in detail the toughening modification of POM by thermoplastic polyester elastomer (TPEE), and the results

Table 1. The compositions of POM/TPEE blends

Sample	1	2	3	4	5	6
POM MC90, phr	100	85	85	85	85	–
TPAE 3533, phr	–	15	15	15	15	100
MAH-*g*-ABS, phr	–	–	0.2	0.4	0.6	–
1010, phr	0.25	0.25	0.25	0.25	0.25	0.25
White oil	Appropriate amount					

showed that TPEE could significantly improve the toughness of POM [16].

Recently, the excellent properties of thermoplastic polyamide elastomer (TPAE) have aroused the research interest of many scholars [17–22]. Like TPU, TPAE materials are also block copolymers that contain hard segments and soft segments. The hard segments can improve processing fluidity and rigidity of TPAE or TPAE blended materials, while soft segments contribute to increasing the toughness of these materials [23–27]. Compared to TPU or other elastomers mentioned above, TPAE not only has better mechanical properties, such as tensile strength, elastic modulus, and notched impact strength, but also has better thermal stability. Therefore, it can be used to improve the impact strength and flexibility at a high or low temperature of other polymers, such as PBT, PET, and so on.

In this paper, MAH-*g*-ABS is used as compatibilizer to improve the compatibility of POM and TPAE, to increase the comprehensive properties of POM/TPAE composites. The POM/TPAE blends with MAH-*g*-ABS are processed by melt extrusion, the content of TPAE elastomer is fixed at 15 phr and the content of MAH-*g*-ABS is 0, 0.2, 0.4, and 0.6 phr respectively. Several analytical and testing methods are used to evaluate the compatibility of MAH-g-ABS on POM/TPAE, such as mechanical properties test, infrared analysis, polarizing microscope test, differential thermal analysis, scanning electron microscope and dynamic mechanical analysis, etc. The results show that MAH-*g*-ABS is a good compatibilizer for toughening and modifying POM with TPAE elastomer.

EXPERIMENTAL

Materials

POM (MC90) was manufactured by Shenhua Co., Ltd, China. TPAE (Pebax 3533) was supplied by Arkema Corporation, France. MAH-*g*-ABS (KT-2) was procured from Shen Yang Ketong Plastic Co., Ltd., China. Antioxidant (Irganox1010) was purchased from Rianlon Corporation, China. White oil (industrial grade 15) was supplied by Petrochina Corporation, China. All the chemicals were commercial grade.

Blend Preparation

POM, TPAE and MAH-*g*-ABS were dried before the extrusion process at 80°C for 4 h to eliminate the residual moisture. The blends were prepared in a twin-screw extruder with the ratio of screw length to diameter equal to 40 and with diameter 26 mm (ZSK26, Coperion GMBH, Germany).

The blends were composed of POM MC90, TPAE 3533, compatibilizer MAH-*g*-ABS, antioxidant, and white oil. To prevent the oxidative degradation of TPAE and POM during melting extrusion, 0.25 wt % Irganox 1010 was added in each experiment. A proper amount of white oil was also needed in order to improve the dispersion of antioxidant. The operating conditions of extrusion were as follows: the temperature of each section of screw was 170/175/180/185/190/190/185/180/175°C; the extrusion load was 15 kg/h; the screw extrusion speed was 300 rpm. The compositions of prepared blends are summarized for clarity in Table 1.

Characterization

Samples for tensile test and notched impact test were prepared by injection molding (HAAKE Mini-Jet-II). The tensile properties of the specimens were tested by Universal Material Testing Machine (INSTRON 5966) according to ISO 527-2 method [28, 29]. The stretching rate was 50 mm/min. The notched impact test was performed according to the ISO 557-2296 standard [30]. All test samples were placed in the Constant Climate Chambers (BINDER, Model KBF 240) for 40 h state adjustment at 23 ± 2°C and 50 ± 5% relative humidity. The above mechanical tests were also performed at 23 ± 2°C and 50 ± 5% relative humidity. The mechanical results were calculated as a function of the original cross section.

FTIR spectra of the specimens were carried out on a BRUKER Vertex 70 FTIR spectrometer (Bruker Daltonics Inc.). The test specimens were made into small pieces of films by using the melt-pressing method operated on the thermal platform [31].

The differential scanning calorimetry (DSC) measurements were carried out by a differential scanning calorimetry (NETZSCH DSC 200F3). Some samples were first heated to 200°C and held for 5 min to eliminate previous thermal history, then cooled down to 30°C subsequently. Both the cooling and heating rates were 10 deg/min. The experiments were carried out under a continuous high purity nitrogen atmosphere [32].

Dynamic mechanical properties of the samples (60 × 10 × 3 mm) were measured under three-point bending mode by a NETZSCH 242E DMA system in a nitrogen atmosphere (50 mL/min). The measured frequency was 5 Hz, and the temperature scan was carried out from −100 to 100°C at a heating rate of 3 deg/min [33].

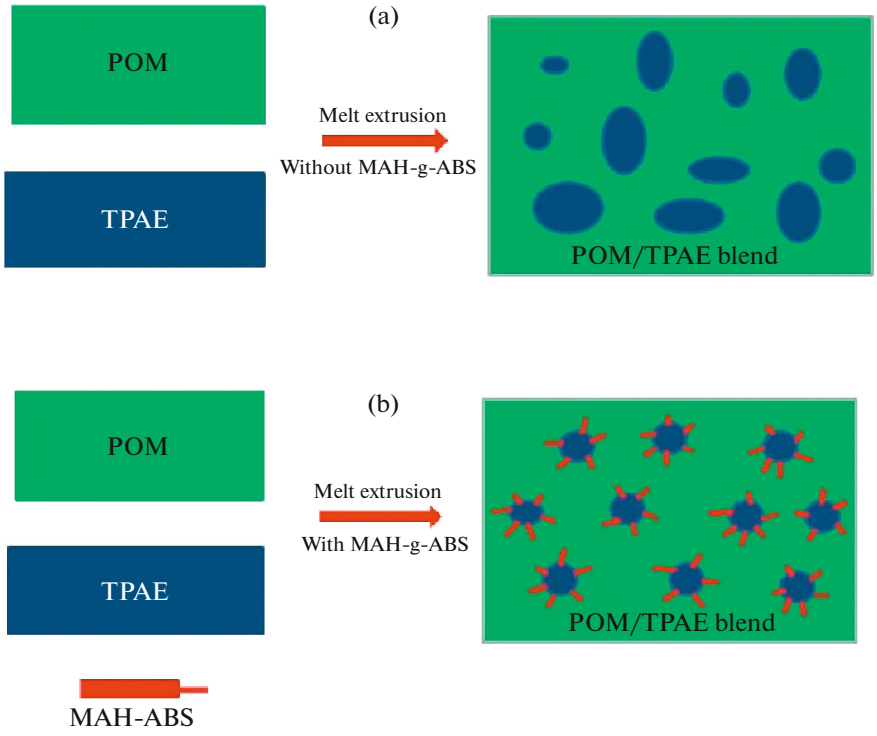

Fig. 1. Compatibility of MAH-*g*-ABS for POM/TPAE blends.

Phenom PRO PW-100-016 scanning electron microscope was used to study morphology of the samples at 10 kV [31]. The sample was fractured in liquid nitrogen, etched by the mixed solvent (the ratio of acetone to chloroform was two to three) at 40°C for 8 h, and then dried in a vacuum at 60°C. The surface of the sample was coated with a thin layer of gold.

A polarized light microscope (PLM) (ZEISSScope.A1, Germany), equipped with a Linkam LTS 420 hot stage (Linkam Scientific Instruments Ltd., Tadworth, UK) was used to study the crystallization process of the POM/TPAE blends. The samples were heated at 200°C for 2 min, then quickly cooled (10 deg/min) to the isothermal crystallization temperature of approximately 147°C. The growth of the spherulites was observed during crystallization using a camera at 200× magnification [34].

RESULTS AND DISCUSSION

In previous studies, we have found that the particle size distribution of "rubber phase" in the composites prepared by simple melt blending of TPAE and POM was uneven, which would affect the toughness of POM/TPAE blends. This phenomenon can be explained by the principle of similarity compatibility [35]. The compatibility law between polymer components can be explained by the following equation: $|\delta A - \delta B| < 1.0$, where δA is the solubility parameter of polymer A, and δB is the solubility parameter of polymer B. If the absolute value of the difference between two parameters is less than 1.0,then two polymers are compatible. If the difference is greater than 1.0, appropriate compatibilizer should be added. The solubility parameter of polyoxymethylene is 20.9 $(J/cm^3)^{1/2}$, and for TPAE it is close to 27.8 $(J/cm^3)^{1/2}$. The difference between them is approximately 6.9 $(J/cm^3)^{1/2}$, so the compatibility of TPAE and POM is not good. In view of the above reasons, it is better to use suitable compatibilizer in the course of preparation of POM/TPAE blends. MAH-*g*-ABS is a good compatibilizer for POM and TPAE, which is because the solubility parameter of ABS is 21.3 $(J/cm^3)^{1/2}$ and that of maleic anhydride is 27.8 $(J/cm^3)^{1/2}$. Figure 1 explains the role of MAH-*g*-ABS in the process of toughening POM by TPAE. TPAE particles in POM/TPAE blends will agglomerate to form more large-size elastomer particles without adding compatibilizer, which is due to the large difference in solubility parameters between POM and TPAE (Fig. 1a). During the melt extrusion of POM/TPAE/MAH-*g*-ABS, the maleic anhydride unit on one side of compatibilizer is compatible with TPAE, while the ABS unit on the other side is compatible with POM. So, after adding MAH-*g*-ABS, the particle size of TPAE elastomer in the blend is more uniform, and no large particles are produced (Fig. 1b).

The tensile strength and elongation at break of POM and POM/TPAE blends with different proportions of compatibilizer are shown in Fig. 2a, from which it can be found that the tensile strength of sam-

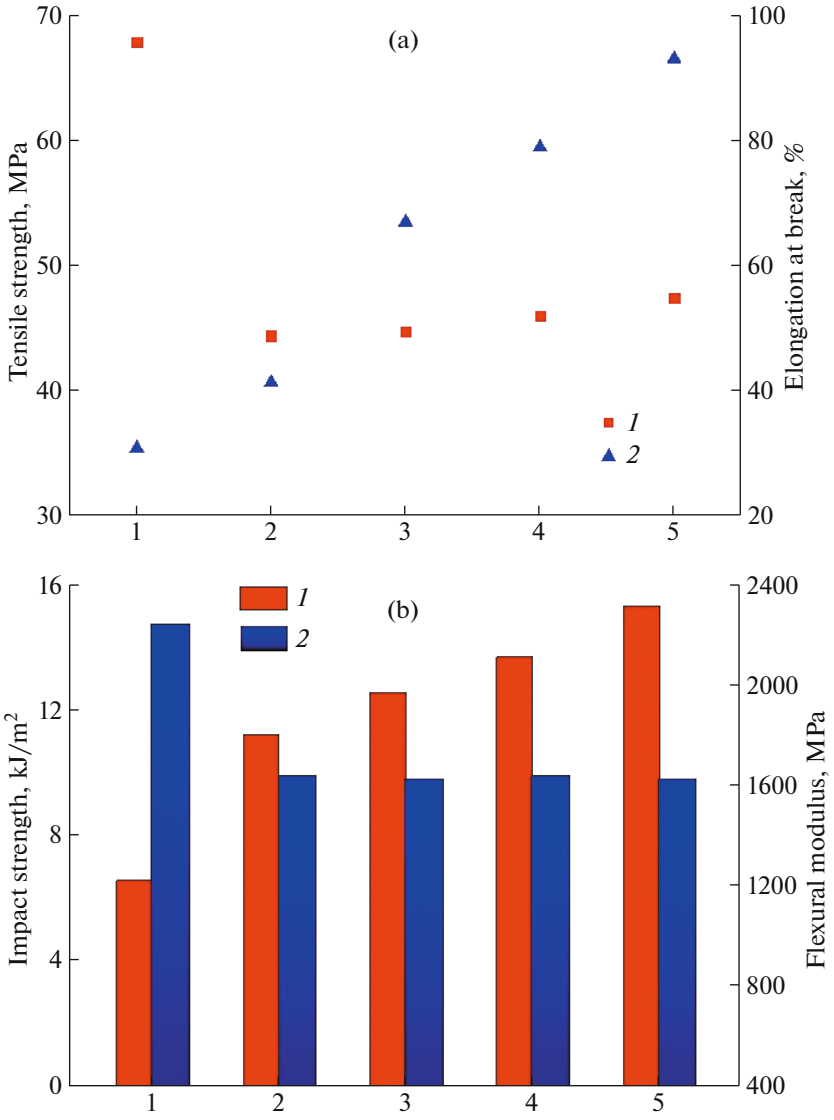

Fig. 2. Mechanical properties of POM/TPAE blends with different amount of compatibilizer: (a) (*1*) tensile strength, (*2*) elongation at break; (b) (*1*) impact strength, (*2*) flexural strength. Formulation of the samples is given in Table 1.

ple 2 with 15 phr TPAE added is lower than that of pure POM, while the elongation at break increases accordingly. When the composition of POM/TPAE is 85/15 and MAH-*g*-ABS compatibilizer is added (samples 3–5), the tensile strength and elongation at break of the blends are improved gradually. For example, compared with sample 2, the tensile strength of sample 5 is increased by 3.0 MPa and elongation at break is increased by 51.9%.

Figure 2b shows that after adding different amount compatibilizer, the impact strength of the blend is significantly improved, but the tensile modulus does not change so much. Contrasted with 2, the notched impact strength of sample 5 is increased by 4.1 kJ/m^2. All these results indicate that MAH-g-ABS has a good compatibility in the preparation of POM/TPAE blends.

Figure 3 compares the FTIR spectra of POM, TPAE and POM/TPAE blends with different amount compatibilizer. In the spectrum of POM MC90, the bands at 2972 and 2912 cm^{-1} are assigned to the CH stretching vibrations; the bands at 1081 and 881 cm^{-1} are assigned to the C–O and C–O–C absorption bands; the band at 632 cm^{-1} is assigned to the OH bending. The FTIR spectrum of TPAE 3533 reveals vibration band of amide bond (NH, 3300 cm^{-1}), of carbon-oxygen double bond (C=O, 1737 cm^{-1}) in saturated polyester segment, carbon-oxygen double bond (C=O, 1640 cm^{-1}) in amide functional group and vibration band of carbon-oxygen-carbon bond (C–O–C, 1094 cm^{-1}). The characteristic bands of

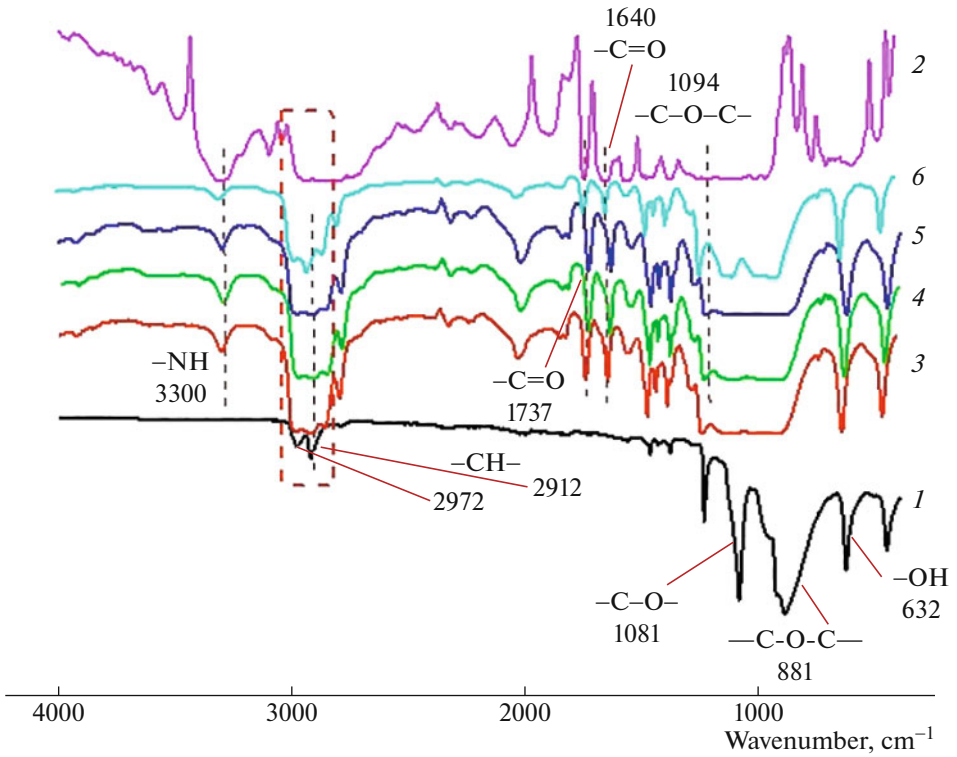

Fig. 3. FTIR spectra of (*1*) POM, (*2*) TPAE and POM/TPAE blends with and without MAH-*g*-ABS: samples (*3*) 2, (*4*) 3, (*5*) 4, (*6*) 5.

both TPAE and POM can be found in FTIR spectrum of their mixture. However, the positions of some characteristic bands are slightly shifted and overlapped. The FTIR spectra of blends with MAH-*g*-ABS are similar to the spectrum of POM/TPAE blend without compatibilizer due to low amount of MAH-*g*-ABS.

Figure 4 shows SEM images of fracture surface morphologies of POM/TPAE thin slice with different compatibilizer loadings. The morphologies of the blends are "sea-island" heterogeneous structures in which the matrix phase is POM resin and the particles phase is TPAE. In addition, it can be found from Fig. 4a that TPAE elastomeric particles present an uneven distribution in POM phase, existing more large elastomeric particles and small elastomeric particles. This is due to the large difference of solubility parameters between TPAE and POM, which results in the agglomeration of some elastomeric particles during the processing.

In the presence of MAH-*g*-ABS, the particle distribution of TPAE elastomer in the POM matrix becomes uniform gradually, and the number of large particles decreases significantly with the increase of compatibilizer dosage (Figs. 4b–4d). The reason is that the compatibility of MAH-g-ABS reduces the probability of TPAE particles agglomerate to form large particles.

The influence of the content of MAH-*g*-ABS on the crystallization behavior of the POM/TPAE blends is evaluated by means of DSC analysis (Fig. 5). As is seen, the crystallization temperature of POM is 143°C and that of TPAE is 59°C, which means the former is easier to crystallize than the latter during the cooling process from high temperature to low temperature. Second the area of crystallization peak of POM is significantly larger than that of TPAE, that is to say the crystallinity of the former is obviously higher than that of the latter. This is because there are some hard segments and most soft segments in the molecular of TPAE, the hard segment is crystalline but the soft segment is amorphous. At last for the POM/TPEE blends with 0.2, 0.4 and 0.6 phr MAH-*g*-ABS, the crystallization temperatures of which are all shifted toward the high temperature zone. But the drift temperature of the above curves is different according to the different amount of compatibilizer. From these curves, we can find that the drift temperature also increases with the content of compatibilizer increases.

In order to study the influence of MAH-g-ABS on the crystal morphology of POM/TPAE blends, we used polarized light microscopy (PLM) (Fig. 6). Figure 6a shows the typical crystal morphology of pure POM resin as large-size spherulitic structure. No crystalline particles are found in Fig. 6b, indicating that TPAE is an amorphous polymer. When the amorphous TPAE is melt blended with POM which is easy

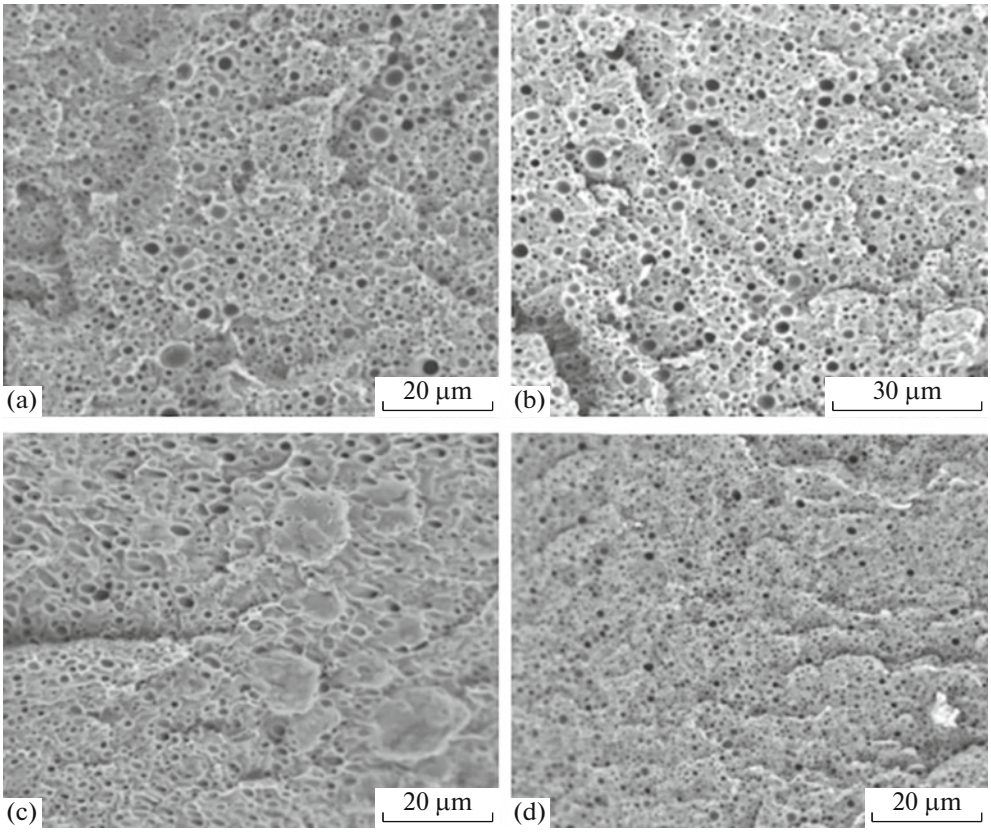

Fig. 4. SEM images of fracture surface morphologies of POM/TPAE/MAH-*g*-ABS blends with different compatibilizer loadings: (a) 0, (b) 0.2, (c) 0.4, (d) 0.6.

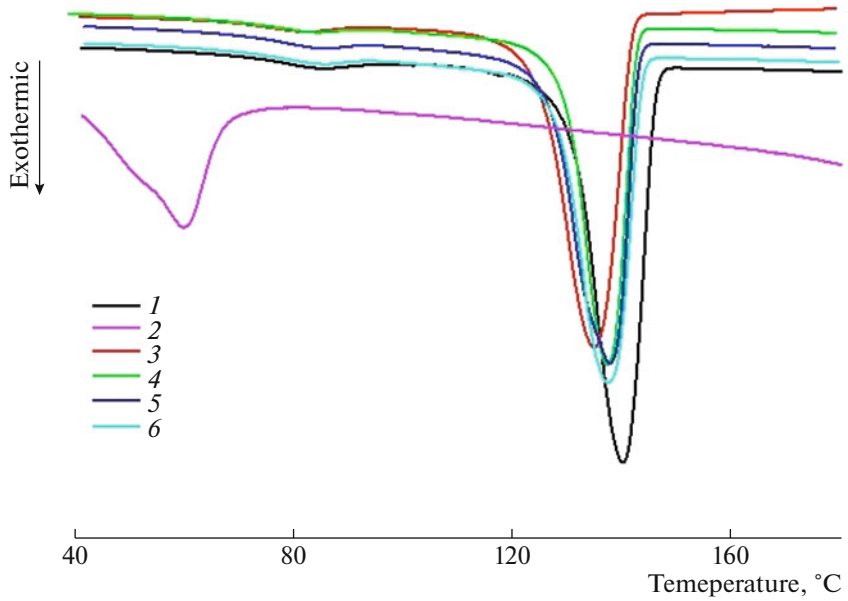

Fig. 5. DCS crystallization exothermic curves of (*1*) POM, (*2*) TPAE, and POM/TPEE blends: samples (*3*) 2, (*4*) 3, (*5*) 4, (*6*) 5.

to crystallize, the crystallinity of POM will be affected, the crystal grains will be smaller or amorphous zone will be produced. As is seen on Fig. 4c the crystallization performance of the blend has decreased and the crystal grains have become smaller. In the presence of MAH-*g*-ABS the crystalline grains of the blends become not very clear, which means that blend matrix produced more amorphous regions during the melting

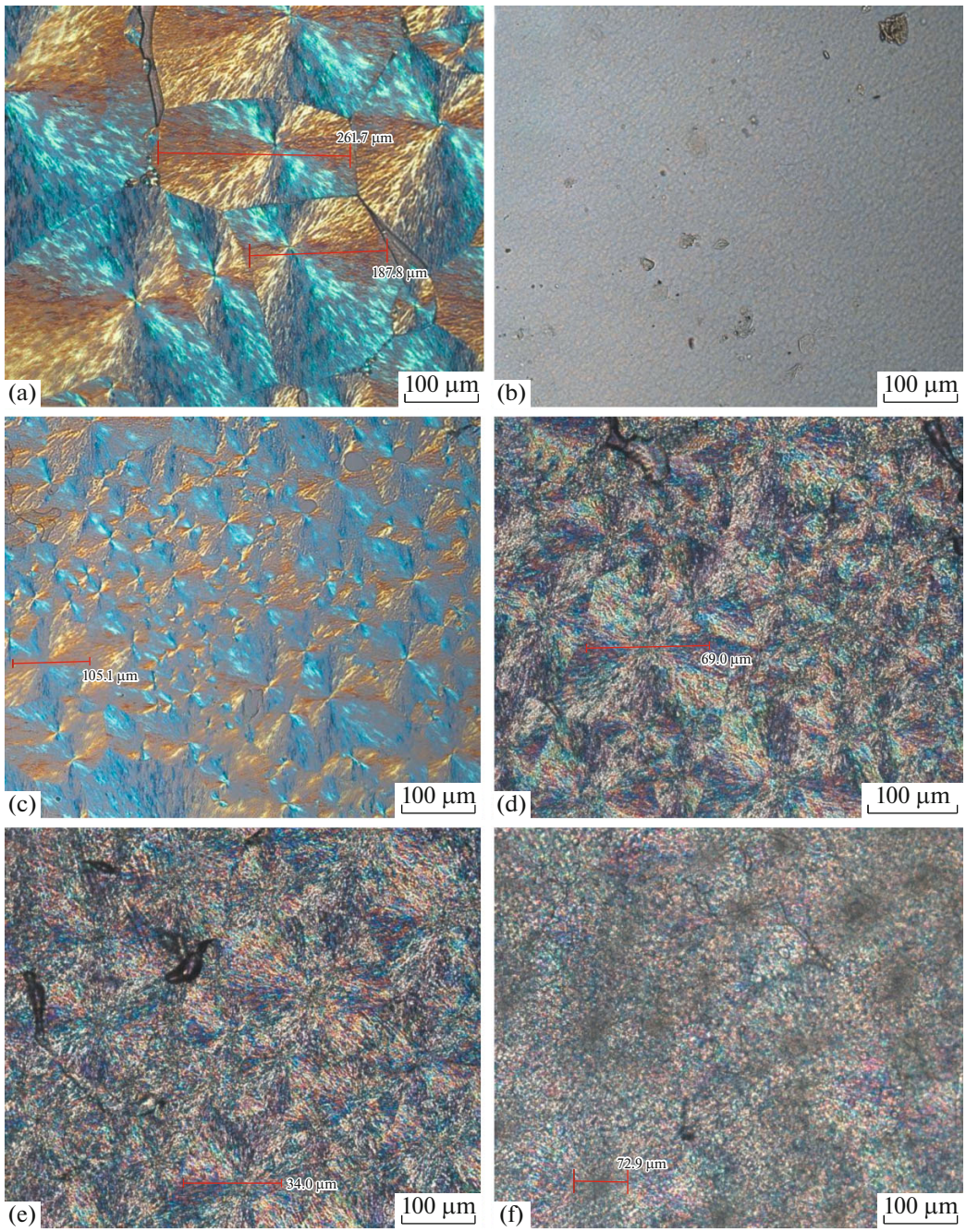

Fig. 6. Polarizing optical micrographs of (a) POM, (b) TPAE, POM/TPAE blends with different MAH-*g*-ABS loadings (c) 0, (d) 0.2, (e) 0.4, (f) 0.6.

and cooling process. From the above analysis, it can be concluded that when preparing POM/TPAE blends, addition of MAH-*g*-ABS can reduce the crystalline area of the composite material and produce more amorphous areas, thereby improving the toughness of the composite materials.

Figure 7 shows that glass transition temperature T_g of the pure TPAE is basically similar to the pure POM, so the vitrification temperature of the POM/TPAE blends has not changed much. The reason for above results is that POM and TPAE have similar molecular flexibility and freedom of segment movement. The loss factor (tan δ) of TPAE is higher than that of POM, and the tan δ of the POM/TPAE blends has intermediate value. This is because TPAE contains amorphous polyether or polyester soft segments, which has viscoelasticity similar to rubber and higher loss modulus, so the loss factor is larger than that of POM. During this testing, an interesting finding is that the

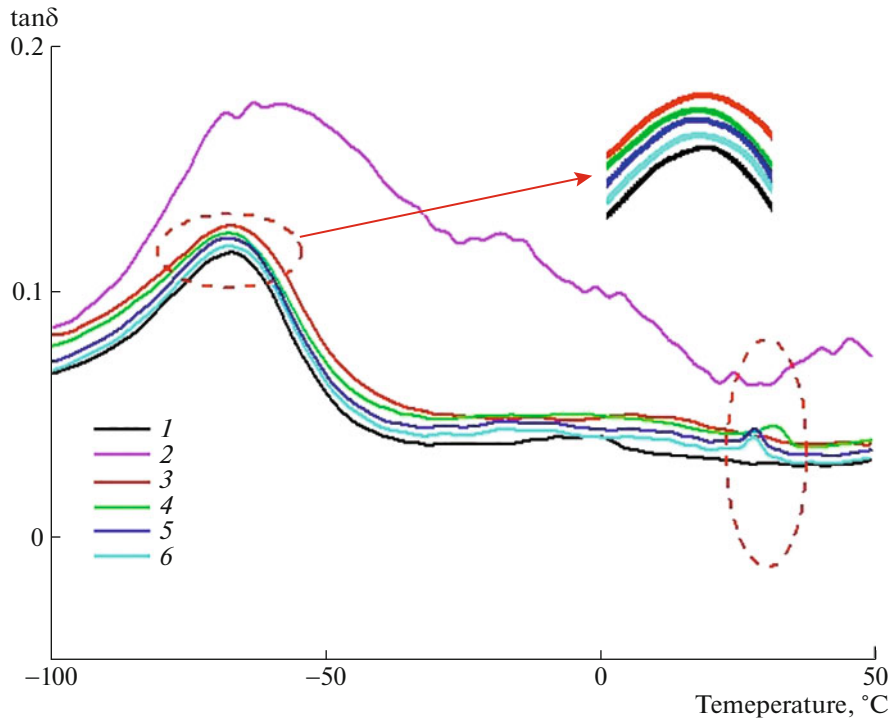

Fig. 7. Temperature dependence of tan δ of (*1*) POM, (*2*) TPAE, and blends with and without MAH-*g*-ABS: samples (*3*) 2, (*4*) 3, (*5*) 4, (*6*) 5.

curves of the blends containing MAH-*g*-ABS contain two loss peaks. First of them is characteristic to POM and TPAE, while the second may be due to the presence of MAH-*g*-ABS.

CONCLUSIONS

The POM/TPAE blends were prepared through melt blending and compatibilized using MAH-*g*-ABS. Characterizations by mechanical testing, SEM, FTIR, PLM, DSC, and DMA were performed to understand the relationship between microstructure and comprehensive properties of the POM/TPAE blends with and without MAH-*g*-ABS. It is found that the elongation at break, notched impact strength and bending modulus of the blends significantly improve with MAH-*g*-ABS loadings. Compared with POM/TPAE, POM/TPAE/MAH-*g*-ABS (75 : 25 : 0.6) sample shows a best toughness, for example, the notched impact strength increases 4.1 kJ/m^2. The SEM observations indicate that the particle distribution of TPAE elastomer in the blend matrix becomes uniform gradually, and the number of large particles decreases significantly with the increase of compatibilizer dosage.

In addition, the nonisothermal crystallization behaviors of POM/TPAE blends with different loadings of MAH-*g*-ABS were investigated by using DSC and PLM. The DCS results indicate that the crystallization temperatures of blends are all shifted toward the high temperature zone with MAH-*g*-ABS loadings. The PLM images show that the crystalline grains of the blends become not very clear which means the blend matrix produced more amorphous regions with MAH-*g*-ABS loadings. All these results indicate that MAH-*g*-ABS is an effective compatibilizer for POM and TPAE.

AUTHOR CONTRIBUTIONS

These authors (Ruilong Li and Wei Fang) contribute equally to this work and share the first authorship.

FUNDING

This work was supported by the 2018 Key R and D Project of Ningxia Hui Autonomous Region (2018BDE02040), China.

CONFLICT OF INTEREST

The authors declare that they have no conflict of interest.

REFERENCES

1. S. Wacharawichanant and T. Siripattanasak, Adv. Chem. Eng. Sci. **3**, 202 (2013).
2. Z. Jiang, Y. Chen, and Z. Liu, J. Polym. Res. **21**, 451 (2014).
3. X. Zheng, C. Zhang, and C. Luo, Ind. Eng. Chem. Res. **55**, 2983 (2016).

4. X. Wang and X. Cui, Eur. Polym. J. **41**, 871 (2005).
5. W. Lin and J.-P. Qu, Ind. Eng. Chem. Res. **58**, 10894 (2019).
6. A. K. Das, S. Suin, N. K. Shrivastava, S. Maiti, J. K. Mishra, and B. B. Khatua, Polym. Compos. **35**, 274 (2014).
7. X. Ren, L. Chen, H. Zhao, Y. Dan, and X.-F. Cai, J. Macromol. Sci. **46**, 411 (2007).
8. D. Zhou, B. You, G. Wu, and X. Ren, Polym. Int. **61**, 971 (2012).
9. M. Hosseinabadi, M. Ghetmiri, A. S. Dindarloo, and Y. Jahani, Polym. Sci., Ser. A **60**, 816 (2018).
10. S. Bai and Q. Wang, J. Vinyl Addit. Technol. **4**, 479 (2016).
11. S. Wacharawichanant, P. Amorncharoen, and R. Wannasirichoke, Key Eng. Mater. **659**, 463 (2015).
12. Y. Liu, T. Zhou, Z. Chen, L. Li, Y. Zhan, A. Zhang, and F. Liu, Polym. Adv. Technol. **25**, 760 (2014).
13. W. Yang, X. L. Wang, and X. Yan, Polym. Eng. Sci. **57**, 1119 (2017).
14. J. Yang, W. Yang, X. Wang, M. Dong, H. Liu, E. K. Wujcik, Q. Shao, S. Wu, T. Ding, and Z. Guo, Macromol. Chem. Phys. **220**, 1800567 (2019).
15. L. Li, D. Xu, and J. Liu, Polym. Mater.: Sci. Eng. **31**, 101 (2015).
16. W. Fang, X. Fan, H. Jiao, and Z. Jin, Polym. Sci., Ser. A **61**, 890 (2019).
17. S. Wang, S. Pang, and L. Pan, Polymers **8**, 417 (2016).
18. S. H. Cho, Y. J. Jang, D. M. Kim, T. Lee, D. Lee, and Y. Lee, Polym. Eng. Sci. **49**, 1456 (2009).
19. J.-M. Lee, B.-H. Choi, J.-S. Moon, and E.-S. Lee, Polym. Test. **28**, 854 (2009).
20. X. Lu, Q. Lv, X. Huang, Z. Song, N. Xu, S. Pang, L. Pan, and T. Li, J. Appl. Polym. Sci. **135**, 46343 (2018).
21. M. Hussain, Y. H. Ko, and Y. H. Choa, J. Nanomater. **2016**, 8515103 (2016).
22. J. Zhan, L. Ma, and X. Liu, Polym.-Plast. Technol. Eng. **56**, 1096 (2017).
23. C. Yi, Z. Peng, H. Wang, M. Li, and C. Wang, Polym. Int. **60**, 1728 (2011).
24. H. Gui, T. Zhou, L. Li, T. Zhou, F. Liu, Y. Zhan, and A. Zhang, J. Appl. Polym. Sci. **130**, 3411 (2013).
25. T. Hao, C. Zhang, and G.-H. Hu, J. Appl. Polym. Sci. **135**, 43337 (2016).
26. D. Chi, F. Liu, and H. Na, ACS Sustainable Chem. Eng. **6**, 9893 (2018).
27. W. Zhou, Y. Zhang, and Y. Xua, Polym. Degrad. Stab. **109**, 21 (2014).
28. J.-M. Lee, B.-H. Choi, J.-S. Moon, and E. S. Lee, Polym. Test. **28**, 854 (2009).
29. S. Yalcın, D. Chateigner, and L. L. Pluart, Mater. Int. **1**, 0029 (2019).
30. A. Rigoussen, P. Verge, and J.-M. Raquez, ACS Sustainable Chem. Eng. **6**, 13349 (2018).
31. S. Wacharawichanant, S. Thongyai, A. Phutthaphan, and C. Eiamsam-ang, Polym. Test. **27**, 971 (2008).
32. F. De Santis, C. Gnerre, M. R. Nobile, and G. Lambretti, Polym. Test. **57**, 971 (2017).
33. X. Guo, J. Zhang, and J. Huang, Polymer **69**, 103 (2015).
34. W. Xu and P. He, Polym. Eng. Sci. **41**, 1903 (2001).
35. S. Abbott, Curr. Opin. Colloid Interface Sci. **48**, 65 (2020).